

# AGILE observations of the ultra-luminous GRB 221009A

*Giovanni Piano<sup>1,\*</sup>, Luca Foffano<sup>1</sup>, and Marco Tavani<sup>1,2</sup>*

<sup>1</sup>INAF-IAPS Roma, via del Fosso del Cavaliere 100, I-00133 Roma, Italy

<sup>2</sup>Dipartimento di Fisica, Università di Roma Tor Vergata, via della Ricerca Scientifica 1, I-00133 Roma, Italy

**Abstract.** The ultra-luminous, long-duration transient event GRB 221009A was detected by several observatories - as the most luminous gamma-ray burst ever observed - from radio to VHE gamma rays, up to tens of TeV. AGILE detected an extraordinary incoming flux of hard X-ray and high-energy gamma-ray photons during this unprecedented event. The high-energy emission (from tens of keV up to GeV energies) has been recorded by the AGILE detectors with an almost-continuous time coverage, monitoring the transition between the prompt and the afterglow phase, up to  $\sim$ 20 ks after the onset of the GRB. AGILE time-resolved spectra and light curves are presented in a multi-frequency context, focused on the observed high-energy component of this intense GRB. The AGILE simultaneous hard-X/gamma-ray observations during the key phases of the burst will be crucial to give robust constraints to the physical evolution of the GRB's high-energy emission.

## 1 Introduction: GRB 221009A, the BOAT

On October 9, 2022 Swift/BAT detected a bright transient emission, subsequently identified as GRB 221009A [1], connected with a core-collapsing massive star at redshift  $z = 0.15095 \pm 0.00005$  [2]. The prompt emission of this long GRB (duration  $\sim$ 600 s) was detected by several satellites [3, 4]. The observations promptly revealed that the event was the brightest GRB ever detected (the brightest of all time, the BOAT). The afterglow emission was monitored by several facilities in the following days up to very-high energy (VHE)  $\gamma$  rays [5]. In this study, we adopt the Fermi-GBM trigger time  $T_0 = 13:16:59.99$  UT [6]. In the following, the time is measured from  $T_0$ .

## 2 The AGILE observations

AGILE [7] observed GRB 221009A with all the active detectors on board the satellite: the gamma-ray imager (GRID) active in the energy band 30 MeV - 50 GeV, the mini calorimeter (MCAL, 350 keV - 10 MeV), and the scientific ratemeters (RMs, 50 - 200 keV) from the anti-coincidence (AC) system, GRID ("unvetoed" signal) and MCAL [8]. The GRB entered for the first time in the GRID field of view (FoV) at  $t \gtrsim 220$  s, during a telemetry saturation of the AC-Top RM induced by the huge incoming X-ray flux (time intervals [220.4, 246.4 s] and [254.4, 272.6 s], see Fig. 1). We excluded from our analysis both the saturation time

\* e-mail: [giovanni.piano@inaf.it](mailto:giovanni.piano@inaf.it)

intervals and corrected, for the remaining dataset, the GRID livetime by taking into account the induced dead time by the RM veto logic. AGILE monitored the evolution of the GRB from the onset of the prompt emission (RMs and MCAL) up to the late afterglow (GRID,  $t \lesssim 20$  ks), accurately observing the transition from the prompt to the afterglow phase (Fig. 2).

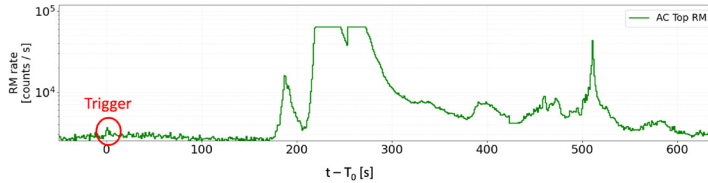


**Figure 1.** Time evolution of the AGILE scientific RMs from the top panel of the AC system, during the GRB 221009A. The red circle indicates the triggering event at  $T_0$ , which turns out to be a weak precursor of the real following burst.

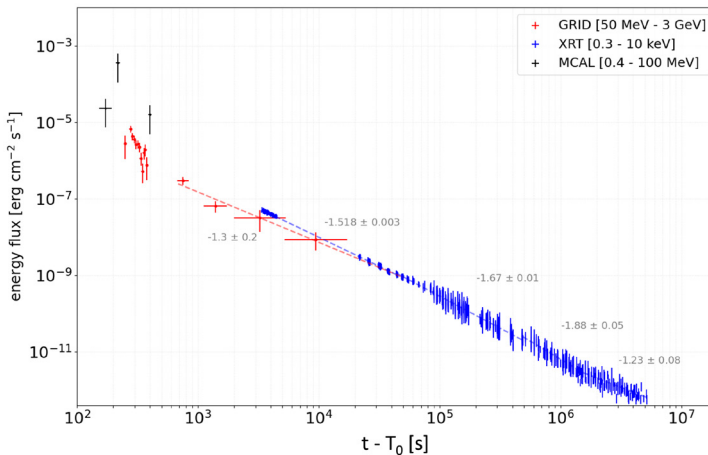


**Figure 2.** Energy flux evolution of the GRB 221009A: prompt phase and afterglow. Black points: AGILE-MCAL. Red points: AGILE-GRID. Blue points: Swift/XRT [9]. Time power-law indices are indicated in the figure.

## 2.1 GRID spectral evolution of the GRB

AGILE monitored GRB 221009A during the transition from the prompt to the afterglow phase. The MeV spectra observed with the MCAL detector sharply indicate a prominent prompt emission during the brightest phase ([210.9, 223.2 s]) with a possible residual component extending up to 481.6 s [8].

The GRID spectral evolution between 50 MeV and 3 GeV is reported in Fig. 3. In Table 1, the resulting parameters of the power-law fits of the analyzed time intervals are reported.

## 3 Modeling the afterglow emission

In order to investigate the afterglow high-energy emission of this extraordinary bright event, we compared simultaneous GeV and TeV  $\gamma$ -ray data from the AGILE-GRID detector and

**Table 1.** Power-law fits of the GRID time intervals.

	Time Intervals [s, s]	Photon Index	Flux photons cm <sup>-2</sup> s <sup>-1</sup>
c1	[273, 303]	$1.9 \pm 0.1$	$(1.5 \pm 0.2) 10^{-2}$
c2	[303, 383]	$2.0 \pm 0.1$	$(5.4 \pm 0.6) 10^{-3}$
d	[684, 834]	$1.7 \pm 0.2$	$(1.1 \pm 0.2) 10^{-3}$
e	[1129, 1279]	$2.1 \pm 0.4$	$(1.7 \pm 0.8) 10^{-4}$
f	[1569, 1719]	$2.5 \pm 0.5$	$(1.0 \pm 0.5) 10^{-4}$

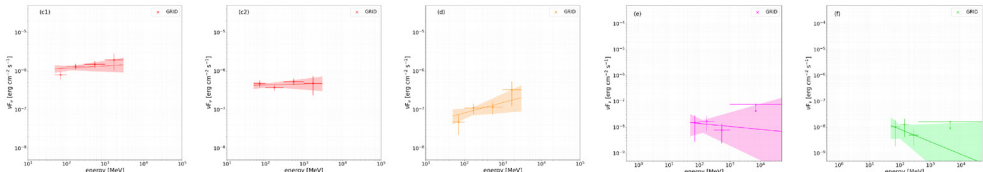


**Figure 3.** AGILE-GRID spectral evolution of the GRB 221009A (50 MeV - 3 GeV). Spectral energy distribution (from left to right) for the c1, c2, d, e, f time intervals. Each spectrum is presented together with the corresponding power-law fit (see Table 1).

the LHAASO observatory, respectively. We performed a specific AGILE data analysis, dividing the observations into time intervals consistent with those reported by the LHAASO Collaboration [5]. In Fig. 4, we show the resulting spectral datasets for the six time intervals considered in this study.

We modeled the experimental data within the relativistic fireball scenario, aiming to describe the broad-band dataset with a consistent theoretical evolution [10]. The model describes the adiabatic expansion of a blast wave into a homogeneous medium. Electrons are accelerated into a power-law distribution with index  $p = 2.5$ , and emit radiation via synchrotron self-Compton process (SSC). The main global parameters adopted in our model include a initial isotropic-equivalent energy of the blast wave of  $E_{\text{iso},0} \simeq 7 \cdot 10^{55}$  erg, an initial bulk Lorentz factor  $\Gamma_0 = 480$ , and a constant density of the surrounding medium  $n_0 = 0.8$  cm<sup>-3</sup>. During the expansion of the blast wave, our model requires time-evolving microphysical parameters  $\varepsilon_e$  and  $\varepsilon_B$ , which describe the fractions of the total shock energy transferred to electrons and magnetic field, respectively.

In Fig. 4, we also show the calculated spectral energy distributions (SEDs) resulting from our model. Our global interpretation of GRB 221009A successfully describes the broad-band non-thermal evolution of the burst, describing the afterglow from early to very late times after the trigger event.

## 4 Conclusions

AGILE observations of the ultra-luminous GRB 221009A represented a crucial opportunity to analyze the evolution of a burst in the MeV-GeV range, following the evolution from the prompt to the afterglow phase. Analyzing the GeV data, collected by the AGILE-GRID detector, simultaneous with the TeV LHAASO data, we found that a single and coherent relativistic fireball model can account for the overall spectral evolution of the GRB during the early afterglow phase of the burst.

AGILE is a mission of the Italian Space Agency (ASI), with scientific and programmatic participation of INAF (Istituto Nazionale di Astrofisica) and INFN (Istituto Nazionale di Fisica Nucleare). This work was partially supported by the grant Addendum No. 7 - Accordo ASI-INAF No. I/028/12/0 for the AGILE project.

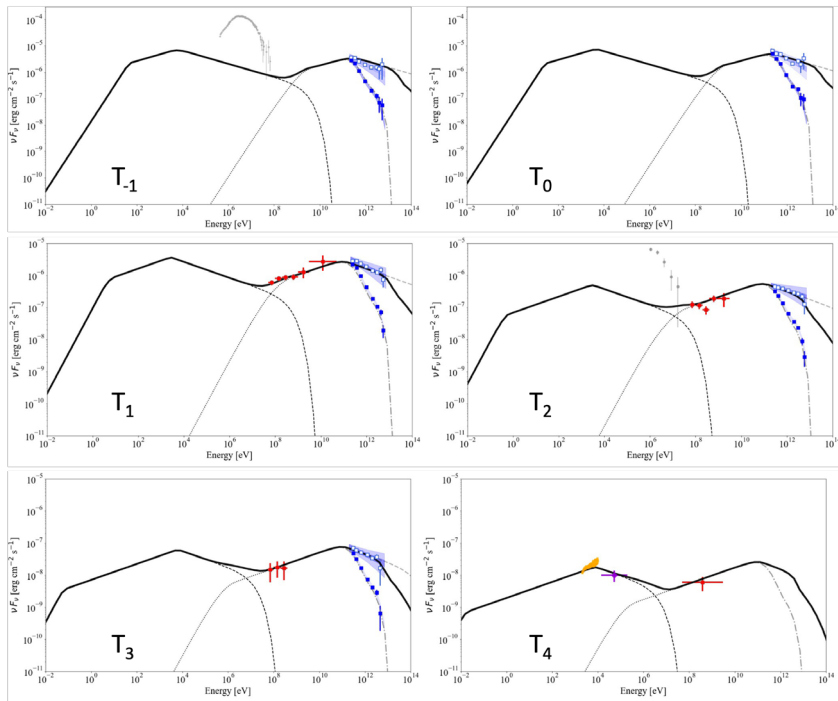


**Figure 4.** Calculated SEDs for the time intervals  $T_{-1} = [231, 240]$  s,  $T_0 = [240, 248]$  s,  $T_1 = [248, 326]$  s,  $T_2 = [326, 900]$  s,  $T_3 = [900, 2000]$  s,  $T_4 = [2014, 5269]$  s. The black continuous thick curve is the overall theoretical SSC emission; the black dashed and dotted curves are the synchrotron and inverse Compton contributions, respectively. The dashed gray curve is the TeV emission without the  $\gamma\gamma$  absorption, and the dashed-dotted gray curve is related to the TeV emission absorbed by the extragalactic background light (EBL). LHAASO data points are reported in blue squares – both the observed data (filled) and the EBL deabsorbed data (empty). The AGILE-GRID data are reported with red circles. X-ray and hard X-ray data from *Swift*/XRT (orange squares), MeV data from AGILE-MCAL data (gray points) [10].

## References

- [1] S. Dichiara, J. D. Groppe, J. A. Kennea, et al., GCN, 32632, 1 (2022)
- [2] A. de Ugarte Postigo, L. Izzo, G. Pugliese, G., GCN, 32648, 1 (2022)
- [3] H. Negoro, M. Nakajima, K. Kobayashi, et al., ATel, 15651, 1 (2022)
- [4] P. Veres, E. Burns, E. Bissaldi, et al., GCN, 32636, 1 (2022)
- [5] Z. Cao, F. Aharonian, Q. An, et al., Science, 380, 1390 (2023)
- [6] S. Lesage, P. Veres, O. J. Roberts, et al., GCN, 32642, 1 (2022)
- [7] M. Tavani, G. Barbiellini, A. Argan, et al., A&A, 502, 995 (2009)
- [8] M. Tavani, G. Piano, A. Bulgarelli, et al., ApJL, 956, L23 (2023)
- [9] M. A. Williams, J. A. Kennea, S. Dichiara, et al., ApJL, 946, L24 (2023)
- [10] L. Foffano, M. Tavani, G. Piano, ApJL, 973, L44 (2024)